pISSN: 2508-5778 • eISSN: 2508-5859
Ann Hepatobiliary Pancreat Surg 2026;30:165-177
https://doi.org/10.14701/ahbps.25-250

AHBPS
Annals of Hepato-Biliary-Pancreatic Surgery

Original Article

Impact of three-dimensional hepatic models on oncological outcomes and survival after hepatectomy: Prognostic factor analysis in a retrospective cohort

María Victoria Vieiro Medina[1], Laura Alonso Murillo[1], Carlos Ernesto García Vasquez[1], Victor Nieto Barros[1], Marta de la Fuente Bartolomé[1], Fernando Neria[2], Santos Francisco Jiménez de los Galanes Marchán[1,2]

[1]Department of General and Digestive Surgery, Infanta Elena University Hospital, Madrid, Spain,
[2]Faculty of Medicine, Universidad Francisco de Vitoria, Madrid, Spain

Backgrounds/Aims: Three-dimensional (3D) modeling is increasingly used in hepatobiliary surgery to enhance anatomical understanding and operative planning. However, its impact on oncologic outcomes remains uncertain. This study evaluated whether preoperative 3D liver models influence resection margin status and survival after hepatectomy for malignant disease.

Methods: In this retrospective case-control study, 59 patients undergoing hepatic resection for malignancy between May 2018 and May 2023 were included. Patients were managed either with patient-specific 3D models (n = 31) or conventional imaging (n = 28). Predictors of R0 resection were analyzed using logistic regression, and overall survival (OS) and disease-free survival (DFS) were assessed using Cox proportional hazards models.

Results: R0 resection was achieved in 79.7% of patients, with no significant difference between groups (77.4% vs. 82.1%; $p = 0.865$). Bilobar tumor distribution (adjusted odds ratio [OR] 0.05, 95% confidence interval [CI] 0.00–0.76; $p = 0.039$) and a higher albumin-bilirubin score (adjusted OR 0.06, 95% CI 0.00–0.46; $p = 0.029$) were independently associated with lower odds of achieving R0 resection. In multivariable analysis, the use of 3D models was independently linked to improved 2-year DFS (adjusted hazard ratio 0.47, 95% CI 0.24–0.92; $p = 0.028$). Tumor type affected recurrence rates, with hepatocellular carcinoma and other tumors showing a lower risk of recurrence compared to colorectal liver metastases. No significant differences in OS were found.

Conclusions: Preoperative 3D modeling was not associated with higher R0 resection rates but was independently associated with improved 2-year DFS. Given the retrospective design and potential residual confounding, these findings should be interpreted cautiously and considered hypothesis-generating pending prospective validation.

Key Words: Hepatectomy; Liver neoplasms; Disease-free survival; Three-dimensional printing; Preoperative care

INTRODUCTION

Three-dimensional (3D) modeling and printing technologies have become invaluable in hepatobiliary surgery. By offering tangible, patient-specific reconstructions of liver anatomy, 3D models improve the understanding of tumor locations, vascular and biliary relationships, and potential resection planes [1-3].

Previous research has indicated that these technologies lead to better operative planning, reduced intraoperative blood loss, and enhanced communication among surgical teams [4,5].

However, current evidence on the impact of 3D printed liver models on oncologic outcomes–such as R0 resection rates and long-term survival–is limited and primarily indirect. Most

Received: December 23, 2025, **Revised:** February 24, 2026,
Accepted: March 13, 2026, **Published online:** April 14, 2026

Corresponding author: María Victoria Vieiro Medina, MD
Department of General and Digestive Surgery, Infanta Elena University Hospital, Avenida de los Reyes Católicos 21, Valdemoro 28342, Madrid, Spain
Tel: +34-918948410, Fax: +34-900606057, E-mail: vickyvieiro@gmail.com
ORCID: https://orcid.org/0000-0002-4421-1825

studies and systematic reviews concentrate on technical accuracy, preoperative planning, and educational benefits rather than directly measuring margin status or recurrence rates [6-10].

A recent meta-analysis of 3D reconstruction-assisted hepatectomy, which included not only physical 3D printed models but also digital 3D visualizations, found that the use of 3D techniques was linked to a lower postoperative recurrence rate (odds ratio [OR] = 0.29, 95% confidence interval [CI]: 0.16–0.53) and a higher postoperative survival rate (OR = 2.19, 95% CI: 1.49–3.23) compared to traditional 2D imaging. This suggests a potential benefit for oncologic outcomes [11]. However, the analysis did not specifically isolate the effects of physical 3D printed models, and most of the included studies did not report R0 resection rates as a primary endpoint.

A preliminary clinical trial utilizing self-healing 3D printed liver models for preoperative planning reported achieving negative surgical margins in all five cases studied. However, the small sample size (n = 5) and lack of long-term survival or recurrence data limit the findings [12]. Other multicenter and systematic studies have confirmed high anatomical fidelity and enhanced intraoperative navigation, but they explicitly indicate that no significant impact on surgical outcomes, including margin status, has been demonstrated to date [6,7,10,13].

Our group has previously examined the effect of 3D modeling on perioperative outcomes in a broader institutional cohort of patients undergoing hepatectomy for both benign and malignant conditions. However, oncologic endpoints were not specifically addressed in that analysis. This prompted the current study, which focuses exclusively on malignant liver tumors and their oncologic outcomes [14].

We hypothesized that the use of patient-specific 3D liver models would improve oncologic outcomes, particularly survival indicators. Therefore, the aim of this study was to evaluate the impact of preoperative 3D modeling on resection margin status and survival outcomes in patients undergoing hepatic resection for malignant disease.

MATERIALS AND METHODS

We conducted a retrospective case-control observational study involving patients who underwent liver resection for malignant disease at Infanta Elena University Hospital (Valdemoro, Madrid) from May 2018 to May 2023. The study included all patients who had oncologic hepatic resection with available preoperative imaging (computed tomography [CT] or magnetic resonance imaging [MRI]) during this period. Patients who underwent urgent procedures or simultaneous resections of other organs were excluded.

Study groups

Patients were divided into two groups according to preoperative planning strategy:

- Group A (control group): surgery performed without a 3D model.
- Group B (3D group): surgery planned using a patient-specific 3D liver model virtual and printed.

Variables and data collection

Variables were grouped into three categories:

Demographic and preoperative variables

Age (years), sex, body mass index (BMI), relevant medical history, presence of steatosis on preoperative ultrasound, and degree of fibrosis measured by preoperative FibroScan were recorded. Functional status was assessed using the Eastern Cooperative Oncology Group (ECOG) [15] scale, the Child-Pugh score [16], and the American Society of Anesthesiologists (ASA) physical status classification [17]. Tumor markers recorded included alpha-fetoprotein, carbohydrate antigen 19-9, and carcinoembryonic antigen. The number and location of lesions were also noted. The albumin-bilirubin score (ALBI) [18] was categorized into three prognostic grades: grade 1 (≤ –2.60), grade 2 (> –2.60 to ≤ –1.39), and grade 3 (> –1.39). Additionally, the tumor burden score (TBS) [19] was classified into three categories: low (< 2.6), intermediate (2.6–7.9), and high (> 7.9).

Intraoperative variables

Surgical approach (laparoscopic, open, or converted) and the type of surgical procedure performed were documented. Hepatic resections were categorized such that any procedure involving at least a segmentectomy was classified as a segmentectomy, even if additional minor resections were performed. Thus, when a segmentectomy was combined with limited resections, the procedure remained classified under the segmentectomy category. Blood loss was recorded in milliliters (mL).

Postoperative variables

The histopathologic diagnosis included the resection margin reported in millimeters. In cases with multiple resected lesions, the margin refers to the smallest distance among all tumors. The percentage of steatosis in the resected specimen was also noted. Margin status was classified as R0 (microscopically negative), R1 (microscopically positive), or R2 (macroscopically incomplete) according to standard pathological criteria [20]. Secondary outcomes included overall survival (OS) and disease-free survival (DFS) at 1 and 2 years.

Acquisition of 3D models

The implementation of 3D modeling started in November 2020. From that point onward, all eligible patients undergoing hepatectomy were routinely planned using 3D models. In contrast, cases prior to November 2020 were treated using traditional two-dimensional imaging. There was no exclusion or selective case assignment based on complexity or surgeon preference. Each model was created from high-resolution CT

and/or MRI datasets using 3D-MSP software (Cella Medical Solutions). Both virtual and printed models were utilized during preoperative planning, with the printed models sterilized for use as intraoperative 3D anatomical references. Fig. 1. illustrates a virtual and printed 3D model overlaid on 2D imaging (CT) of a patient with bilobar colorectal liver metastases (CRLM).

Surgical technique

All hepatic resections were performed using an ultrasonic surgical aspirator and the Aquamantys system. Intraoperative ultrasound (IOUS) was routinely conducted in every case. The type of resection was determined based on tumor type, number, and extension.

Statistical analysis

Continuous variables were reported as median and interquartile range, expressed as "Q3–Q1", and were compared using the Mann–Whitney U test (Wilcoxon rank-sum test).

Categorical variables were presented as absolute and relative frequencies and were compared using the chi-squared test or Fisher's exact test, as appropriate.

Variables with a p-value < 0.2 in univariate analysis were considered for inclusion in the multivariable models. Additionally, the variable "3D model use" was included in all multivariable models, regardless of its univariate significance, as it represented the primary exposure of interest. The final model was derived using backward stepwise selection based on the Akaike Information Criterion.

OS and DFS were illustrated using Kaplan-Meier curves for each group.

Univariate and multivariable Cox proportional hazards regression analyses were conducted to identify factors associated with survival. Survival estimates were compared using hazard ratios (HRs) with 95% CIs.

A p-value < 0.05 was considered statistically significant.

Statistical analysis was conducted using R software (version 4.4). The data exhibited high completeness across all included covariates, with missing data minimal (< 5% for all variables). Due to this low percentage of missing data and to enhance model interpretability, we employed complete case analysis (listwise deletion) to handle the missing values. Participants with any missing values among the variables selected for the final multivariable model were excluded from the regression analysis. This method ensured that the final model was based on a consistent subset of patients, eliminating the need for data imputation.

Ethical considerations

The study received approval from the Research Ethics Committee of the Fundación Jiménez Díaz University Hospital (CEIm EO261-23_HIE, approval date: January 8, 2024), in accordance with the principles of the Declaration of Helsinki. A waiver of informed consent was requested from the Ethics Committee.

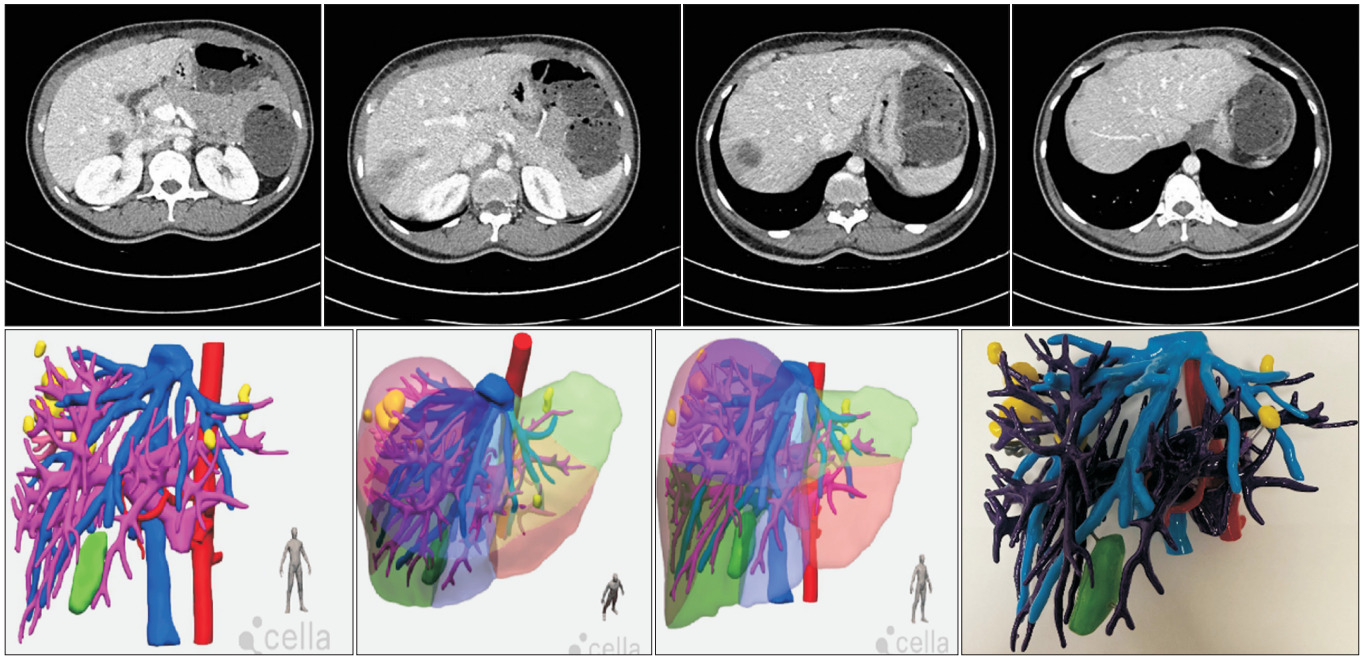

Fig. 1. Two-dimensional (2D) computed tomography imaging with overlaid virtual and printed 3D models for a patient with bilobar colorectal liver metastases.

RESULTS

Between May 2018 and May 2023, a total of 72 patients underwent oncologic hepatic resection at Infanta Elena University Hospital in Valdemoro, Madrid. Thirteen patients were excluded due to urgent procedures or simultaneous resection of another organ, leaving 59 patients for analysis. The patients were divided into two groups: those without a preoperative 3D model (group A, n = 28) and those with a 3D model (group B, n = 31) (Fig. 2).

Development of the 3D model

The average production cost for both the virtual and printed 3D models ranged from €1,500 to €2,300, with a median of €1,800 (€1,600–€2,100). The average production time was less than 12 hours for the virtual model, while the printed model required a median of 40 hours (22–50 hours).

Demographic and preoperative characteristics

No significant differences were observed between groups, except for the presence of dyslipidemia, which was higher in the control group (p = 0.032). All patients were classified as Child-Pugh class A. Most patients had an ECOG performance status of 0 (n = 55, 93.2%), while only four patients were classified as ECOG 1 (6.8%). ASA class II and III represented the most frequent anesthetic risk categories. A similar proportion of patients in both groups received neoadjuvant chemotherapy (55.6% in group A vs. 67.7% in group B; p = 0.34). ALBI grade 1 was the most common category (n = 41, 69.5% of the total), and the intermediate TBS category was also predominant (n = 28, 50.9%). Baseline demographic and preoperative characteristics of the 59 patients were comparable between groups (Table 1).

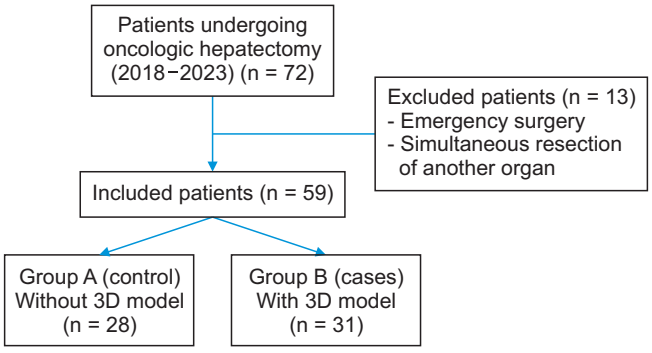

Fig. 2. Study flow diagram. Of the 72 consecutive patients who underwent oncologic hepatic resections, thirteen were excluded for having simultaneous organ resections or requiring emergency surgery. The remaining 59 patients were divided into two groups: those without preoperative three-dimensional (3D) simulation (group A, no 3D model) and those with preoperative 3D simulation (group B, 3D model).

Surgical procedure and intraoperative findings

Regarding the surgical approach, open hepatectomy was performed in 30 patients (50.8%), while 28 patients (47.5%) underwent a laparoscopic approach, and one patient (1.7%) required conversion from laparoscopy to open surgery. The distribution of surgical approaches differed slightly between groups, with laparoscopic resection being more frequent in the 3D group (58.1%) than in the non-3D group (35.7%), although the difference did not reach statistical significance (p = 0.086).

Intraoperative blood loss showed a significant difference between groups (p < 0.001). The median was 250.0 mL (175.0–325.0 mL), compared with 287.5 mL (250.0–362.5 mL) in the non-3D group and 175.0 mL (100.0–250.0 mL) in the 3D-model group.

The rest of the surgical procedure and the intraoperative findings were comparable between groups; these findings are summarized in Table 2.

Posoperative outcomes

Pathological findings

Regarding hepatic steatosis, 53.1% of patients had no steatosis (< 5%), 32.7% had mild steatosis (5%–33%), and 14.3% had moderate steatosis (34%–66%). No cases of severe steatosis (> 66%) were observed. When categorized as none/mild versus moderate/severe, 85.7% of patients fell into the first category, while 14.3% fell into the second. No statistically significant differences were found between the groups with and without 3D models, both in the distribution of steatosis (p = 0.577) and in the combined category (p > 0.999).

The mean resection margin was 6.2 ± 9.6 mm, with a median of 2.3 mm (0.9–6.0). No significant differences were observed between the groups without 3D models (mean 7.7 ± 12.1 mm, median 2.7 [1.1–6.9]) and those with 3D models (mean 4.9 ± 6.5 mm, median 2.0 [0.4–5.7]; p = 0.698).

Regarding surgical margin status, 79.7% of patients achieved R0 resection, while 16.9% and 3.4% corresponded to R1 and R2, respectively. No significant differences were observed between the groups (R0: 82.1% vs. 77.4%; p = 0.865).

In the postoperative diagnosis, CRLM were the most frequent at 57.6%, followed by hepatocellular carcinoma (HCC, 20.3%), intrahepatic cholangiocarcinoma (10.2%), and less common neoplasms such as gallbladder or perihilar cholangiocarcinoma (pCCA), gastrointestinal stromal tumor metastases, and neuroendocrine tumors. No significant differences were observed in the distribution of diagnoses between patients who underwent 3D model planning and those who did not (p = 0.218). When the diagnoses were categorized into three groups (colorectal metastases, HCC, and others), no significant differences were noted among the groups (p = 0.532).

Overall, the pathological findings were comparable between patients who had 3D planning and those who did not, with no statistically significant differences in steatosis, resection margins, or lesion type. Histopathological analysis revealed similar

Table 1. Demographic and preoperative characteristics

	Overall (N = 59)	3D model		*p*-value[a)]
		No (N = 28)	Yes (N = 31)	
Age				0.523
Mean ± SD	63.6 ± 11.3	64.9 ± 10.2	62.5 ± 12.2	
Median (IQR)	63.0 (56.0–72.0)	63.5 (57.5–72.5)	61.0 (53.0–72.0)	
Sex				0.158
Female	16 (27.1)	10 (35.7)	6 (19.4)	
Male	43 (72.9)	18 (64.3)	25 (80.6)	
BMI				0.903
Mean ± SD	28.19 ± 4.88	28.16 ± 5.26	28.22 ± 4.60	
Median (IQR)	28.37 (24.75–30.86)	27.41 (24.39–32.03)	28.41 (25.39–29.90)	
Diabetes mellitus	11 (18.6)	8 (28.6)	3 (9.7)	0.063
Hypertension	35 (59.3)	18 (64.3)	17 (54.8)	0.461
Dyslipidemia	12 (20.3)	9 (32.1)	3 (9.7)	0.032*
Arrhythmia/valvular disease	3 (5.1)	2 (7.1)	1 (3.2)	0.599
Respiratory history	12 (20.3)	8 (28.6)	4 (12.9)	0.135
Steatosis on ultrasound	12 (30.0)	8 (38.1)	4 (21.1)	0.240
Not available	19	7	12	
FibroscanPre				0.350
F0-1 (< 8.2 kPa)	2 (20.0)	1 (33.3)	1 (14.3)	
F2 (8.2–9.7 kPa)	3 (30.0)	0 (0.0)	3 (42.9)	
F3 (9.7–13.6 kPa)	2 (20.0)	0 (0.0)	2 (28.6)	
F4 (> 13.6 kPa)	3 (30.0)	2 (66.7)	1 (14.3)	
Not available	49	25	24	
ECOG				0.614
ECOG 0	55 (93.2)	27 (96.4)	28 (90.3)	
ECOG 1	4 (6.8)	1 (3.6)	3 (9.7)	
Child-Pugh score				0.409
5	53 (89.8)	24 (85.7)	29 (93.5)	
6	6 (10.2)	4 (14.3)	2 (6.5)	
Preoperative chemotherapy	36 (62.1)	15 (55.6)	21 (67.7)	0.340
Not available	1	1	0	
ASA				0.238
ASA 1	1 (1.7)	1 (3.6)	0 (0.0)	
ASA 2	29 (49.2)	11 (39.3)	18 (58.1)	
ASA 3	29 (49.2)	16 (57.1)	13 (41.9)	
AFP preoperative				> 0.999
Mean ± SD	19.3 ± 52.0	5.8 ± 4.7	26.1 ± 63.9	
Median (IQR)	2.5 (1.9–8.8)	5.5 (1.8–9.8)	2.5 (2.0–7.1)	
Not available	47	24	23	
Alfafeto postoperative				0.669
Mean ± SD	2.9 ± 2.2	2.9 ± 2.7	3.0 ± 2.0	
Median (IQR)	1.9 (1.6–3.5)	1.7 (1.5–4.4)	2.2 (1.6–3.5)	
Not available	49	4	25	
CEA preoperative				0.509
Mean ± SD	21.1 ± 72.5	27.3 ± 90.1	13.5 ± 43.4	
Median (IQR)	3.1 (1.9–5.4)	4.1 (1.8–5.4)	2.9 (2.1–4.4)	
Not available	21	7	14	

Table 1. Continued

	Overall (N = 59)	3D model		*p*-value[a]
		No (N = 28)	Yes (N = 31)	
CEA postoperative				0.161
Mean ± SD	16.8 ± 65.8	29.0 ± 88.6	2.4 ± 1.2	
Median (IQR)	2.7 (1.6–4.2)	3.4 (1.4–7.5)	2.5 (1.7–2.9)	
Not available	22	8	14	
Ca19-9 preoperative				> 0.999
Mean ± SD	369.1 ± 969.0	487.7 ± 1,160.4	92.3 ± 145.3	
Median (IQR)	13.0 (9.0–186.0)	12.0 (9.0–186.0)	14.0 (3.0–260.0)	
Not available	49	21	28	
Ca19-9 postoperative				0.931
Mean ± SD	16.7 ± 18.1	16.7 ± 17.3	16.8 ± 21.2	
Median (IQR)	10.0 (2.1–29.0)	9.5 (4.0–29.0)	10.0 (2.1–17.0)	
Not available	48	22	26	
Number of lesions				0.741
Mean ± SD	2.1 ± 2.1	1.9 ± 2.1	2.2 ± 2.2	
Median (IQR)	1.0 (1.0–2.0)	1.0 (1.0–2.0)	1.0 (1.0–3.0)	
Localization				0.737
Single	36 (61.0)	17 (60.7)	19 (61.3)	
2–4	17 (28.8)	9 (32.1)	8 (25.8)	
> 5	6 (10.2)	2 (7.1)	4 (12.9)	
Extention				0.915
Unilobar	46 (78.0)	22 (78.6)	24 (77.4)	
Bilobar	13 (22.0)	6 (21.4)	7 (22.6)	
Tumor type				0.573
Primary	21 (35.6)	11 (39.3)	10 (32.3)	
Metastatic	38 (64.4)	17 (60.7)	21 (67.7)	
ALBI_cat				0.149
ALBI grade 1	41 (69.5)	17 (60.7)	24 (77.4)	
ALBI grade 2	17 (28.8)	11 (39.3)	6 (19.4)	
ALBI grade 3	1 (1.7)	0 (0.0)	1 (3.2)	
TBS_cat				0.669
TBS low	22 (40.0)	8 (33.3)	14 (45.2)	
TBS intermediate	28 (50.9)	14 (58.3)	14 (45.2)	
TBS high	5 (9.1)	2 (8.3)	3 (9.7)	
Not available	4	4	0	

Values are presented as number only or number (%).
3D, three-dimensional; SD, standard deviation; IQR, interquartile range; BMI, body mass index; ECOG, Eastern Cooperative Oncology Group performance status; ASA, American Society of Anesthesiologists physical status classification; AFP, alpha-fetoprotein; CEA, carcinoembryonic antigen; Ca19-9, carbohydrate antigen 19-9; ALBI, albumin-bilirubin score; TBS, tumor burden score.
[a]Wilcoxon rank sum test; Pearson's chi-squared test; Fisher's exact test; Wilcoxon rank sum exact test.
*Statistically significant difference ($p < 0.05$).

tumor types and sizes, with a predominance of CRLM (Table 3).

Multivariate analysis for R0 resection

In the multivariate analysis, two variables were independently associated with the likelihood of achieving an R0 resection: bilobar tumor distribution and ALBI score.

Patients with bilobar tumor involvement had a significantly lower probability of achieving negative margins (adjusted OR 0.05, 95% CI 0.00–0.76; $p = 0.039$). Similarly, higher ALBI scores were linked to reduced odds of R0 resection (adjusted OR 0.06, 95% CI 0.00–0.46; $p = 0.029$).

The use of 3D surgical models was not significantly associated with R0 resection rates ($p > 0.05$). Likewise, other evaluated variables–including the number of lesions, BMI, sex, surgical approach, and degree of steatosis–did not show significant associations after multivariable adjustment (Table 4).

Table 2. Surgical procedure and intraoperative findings

	Overall (N = 59)	3D model		*p*-value[a]
		No (N = 28)	Yes (N = 31)	
Surgical approach				0.069
Open	30 (50.8)	18 (64.3)	12 (38.7)	
Laparoscopic	28 (47.5)	10 (35.7)	18 (58.1)	
Converted laparoscopy	1 (1.7)	0 (0.0)	1 (3.2)	
Approach_cat				0.086
Open/converted laparoscopy	31 (52.5)	18 (64.3)	13 (41.9)	
Laparoscopic	28 (47.5)	10 (35.7)	18 (58.1)	
Type of surgery				0.790
Single limited resection	20 (33.9)	9 (32.1)	11 (35.5)	
Multiple limited resection	17 (28.8)	7 (25.0)	10 (32.3)	
Bisegmentectomy	11 (18.6)	6 (21.4)	5 (16.1)	
Segmentectomy	5 (8.5)	2 (7.1)	3 (9.7)	
Right hemihepatectomy	2 (3.4)	2 (7.1)	0 (0.0)	
Left hemihepatectomy	3 (5.1)	1 (3.6)	2 (6.5)	
Extended right hepatectomy	1 (1.7)	1 (3.6)	0 (0.0)	
Resection type_cat				0.401
Limited	37 (62.7)	16 (57.1)	21 (67.7)	
Anatomic	22 (37.3)	12 (42.9)	10 (32.3)	
Blood loss (mL)				< 0.001*
Mean ± SD	269.5 ± 159.7	345.5 ± 169.2	200.8 ± 115.4	
Median (IQR)	250.0 (175.0–325.0)	287.5 (250.0–362.5)	175.0 (100.0–250.0)	

Values are presented as number (%).
3D, three-dimensional; SD, standard deviation; IQR, interquartile range.
[a]Fisher's exact test; Pearson's chi-squared test.
*Statistically significant difference ($p < 0.05$).

Overall survival and disease-free survival

No significant differences were observed between group A (without the 3D model) and group B (with the 3D model) regarding OS or DFS at one and two years. Kaplan-Meier survival curves are presented in Fig. 3.

Overall survival

At 1-year, univariate analysis indicated that bilobar tumor involvement and higher intraoperative blood loss were associated with reduced OS; however, a multivariable analysis could not be conducted due to the low number of events (n = 4).

At 2 years, R1/R2 resection, bilobar involvement, and blood loss were associated with worse OS in the univariate analysis. In the multivariable model, R1/R2 resection and intraoperative blood loss remained independent predictors of decreased 2-year survival.

Disease-free survival

At 1-year, univariate analysis indicated that R1/R2 resection, higher TBS, and increased intraoperative blood loss were associated with reduced DFS. In the multivariable model, R1/R2 resection remained the strongest independent predictor of early recurrence, while intraoperative blood loss also retained statistical significance.

At two years, univariate analysis identified R1/R2 resection, higher TBS, and intraoperative blood loss as predictors of recurrence. In multivariable analysis, higher BMI was associated with a lower risk of recurrence, and preoperative use of 3D models was independently linked to improved two-year DFS. Additionally, postoperative diagnosis influenced outcomes, with HCC and other tumor types showing a lower recurrence risk compared to colorectal metastases. R1/R2 resection continued to be strongly associated with worse two-year DFS.

TBS was not included in multivariable models due to its inability to be calculated for four patients–one with pCCA and three with gallbladder carcinomas–resulting in over 5% missing data. Consequently, TBS was analyzed only in univariate models. Table 5 summarizes the univariate and multivariable analyses for overall and DFS at one and two years.

DISCUSSION

This retrospective study offers a comprehensive assessment of the role of 3D hepatic models in patients undergoing hepa-

Table 3. Pathological findings

	Overall (N = 59)	3D model		*p*-value[a)]
		No (N = 28)	Yes (N = 31)	
Steatosis on histopathology				0.577
None (< 5%)	26 (53.1)	12 (46.2)	14 (60.9)	
Mild (5%–33%)	16 (32.7)	10 (38.5)	6 (26.1)	
Moderate (34%–66%)	7 (14.3)	4 (15.4)	3 (13.0)	
Severe (> 66%)	0 (0.0)	0 (0.0)	0 (0.0)	
Not available	10	2	8	
Steatosis on histopathology_cat				> 0.999
None/mild	42 (85.7)	22 (84.6)	20 (87.0)	
Moderate/severe	7 (14.3)	4 (15.4)	3 (13.0)	
Not available	10	2	8	
Margin (mm)				0.698
Mean ± SD	6.2 ± 9.6	7.7 ± 12.1	4.9 ± 6.5	
Median (IQR)	2.3 (0.9–6.0)	2.7 (1.1–6.9)	2.0 (0.4–5.7)	
Margin state				0.865
R0	47 (79.7)	23 (82.1)	24 (77.4)	
R1	10 (16.9)	4 (14.3)	6 (19.4)	
R2	2 (3.4)	1 (3.6)	1 (3.2)	
R0				0.653
R0	47 (79.7)	23 (82.1)	24 (77.4)	
R1/R2	12 (20.3)	5 (17.9)	7 (22.6)	
Postoperative diagnosis				0.218
CRC metastasis	34 (57.6)	17 (60.7)	17 (54.8)	
HCC	12 (20.3)	4 (14.3)	8 (25.8)	
iCCA	6 (10.2)	3 (10.7)	3 (9.7)	
Gallbladder carcinoma	3 (5.1)	3 (10.7)	0 (0.0)	
Metastasis GIST	2 (3.4)	0 (0.0)	2 (6.5)	
pCCA	1 (1.7)	1 (3.6)	0 (0.0)	
Metastasis NET	1 (1.7)	0 (0.0)	1 (3.2)	
Postoperative diagnosis_cat				0.532
CRC metastasis	34 (57.6)	17 (60.7)	17 (54.8)	
HCC	12 (20.3)	4 (14.3)	8 (25.8)	
Others tumors	13 (22.0)	7 (25.0)	6 (19.4)	

Values are presented as number only or number (%).
3D, three-dimensional; SD, standard deviation; IQR, interquartile range; CRC, colorectal cancer metastasis; HCC, hepatocellular carcinoma; iCCA, intrahepatic colangiocarcinoma; GIST, intestinal gastrointestinal stromal tumor; pCCA, perihiliar colangiocarcinoma; NET, neuroendocrine tumor.
[a)]Fisher's exact test; Wilcoxon rank sum test; Pearson's chi-squared test.

Table 4. Multivariate model for R0 resection

	Univariate					Multivariate (adjusted)		
	N	Event N	OR	95% CI	*p*-value	OR	95% CI	*p*-value
3D-model		24	0.75	0.20, 2.67	0.653	0.19	0.01, 1.40	0.141
Bilobar		8	0.29	0.07, 1.18	0.076	0.05	0.00, 0.76	0.039*
ALBI	59	47	0.18	0.03, 0.84	0.041*	0.06	0.00, 0.46	0.029*

3D, three-dimensional; OR, odds ratio; CI, confidence interval; ALBI, albumin-bilirubin score.
*Statistically significant difference ($p < 0.05$).

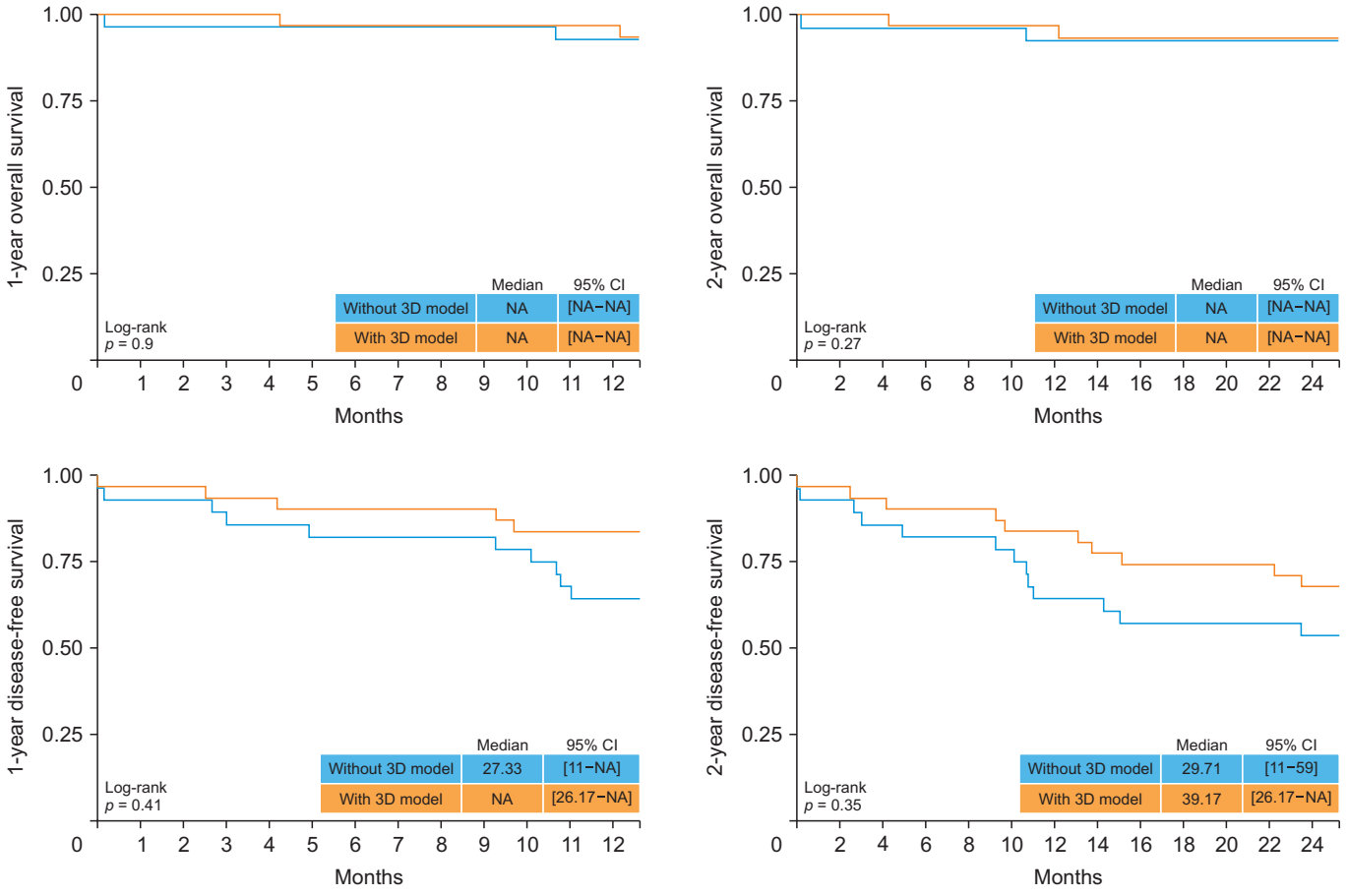

Fig. 3. Overall survival and disease-free survival. Kaplan-Meier survival curves 1 and 2 year overall survival and 1 and 2 year disease-free survival. 3D, three-dimensional; NA, not available; CI, confidence interval.

tectomy for malignant disease. It focuses not only on oncologic outcomes but also on feasibility, perioperative behavior, and pathological characteristics. Our findings indicate that while 3D models did not improve R0 resection rates, their use was independently associated with enhanced 2-year DFS. This contribution is significant, as most published reports emphasize the technical advantages of 3D modeling–such as improved anatomical understanding, operative planning, and communication within surgical teams–rather than its long-term oncologic implications [1-10]. Notably, unlike many studies that rely solely on digital reconstructions, our workflow incorporated both virtual and sterilizable printed 3D models. This approach allowed surgeons to physically interact with patient-specific anatomy and use the printed model as an intraoperative spatial reference. This dual-modality method may partially explain the enhanced anatomical comprehension observed in the 3D group. The implementation of 3D models was feasible within our clinical workflow, with production times and costs aligning with previously reported multicenter experiences [6,8,9]. Baseline demographic and clinical characteristics were balanced between the groups, which reduces the likelihood of selection bias and strengthens the internal validity of the comparative analyses.

Perioperatively, patients in the 3D group experienced significantly lower intraoperative blood loss. This finding aligns with recent meta-analyses that demonstrate improved anatomical precision and reduced surgical complexity when using 3D planning [21-23]. These results support the safety and potential operational advantages of integrating 3D modeling into preoperative planning, without changing surgical indications or increasing procedural aggressiveness.

Pathological findings showed no significant differences between groups regarding steatosis, tumor type, lesion distribution, or resection margin width. The predominance of CRLM in our cohort aligns with contemporary case-mix patterns and is consistent with the literature, where CRLM is the most common indication for oncologic liver resection, accounting for up to 64% of hepatic resections [24,25].

The lack of differences in R0 resection rates between groups aligns with previous reports indicating that margin negativity is primarily influenced by IOUS, tumor biology, and anatomic complexity, rather than solely by preoperative planning tools

Table 5. Univariate and multivariate Cox proportional hazards regression to identify factors associated with overall and disease-free survival at one and two years

	Univariate					Multivariate (ajusted)		
	N	Event N	HR	95% CI	*p*-value	HR	95% CI	*p*-value
One-year OS								
Bilobar		3	12.1	1.25, 116	0.031*			
Blood loss	59	4	1.01	1.00, 1.01	0.018*			
Two-year OS								
Bilobar		5	3.57	1.09, 11.7	0.036*			
Blood loss	59	11	1	1.00, 1.01	< 0.001*	1	1.00, 1.01	0.012*
R1/R2		6	6.6	2.00, 21.7	0.002*	8.61	1.73, 43.0	0.009*
One-year DFS								
Blood loss	59	27	1	1.00, 1.01	0.004*	1	1.00, 1.01	0.009*
TBS	55	26	1.19	1.04, 1.37	0.014*			
R1/R2		10	5.59	2.51, 12.5	< 0.001*	6.05	2.60, 14.1	< 0.001*
Two-year DFS								
BMI	59	41	0.95	0.88, 1.02	0.134	0.88	0.81, 0.96	0.003*
3D-model		20	0.75	0.40, 1.38	0.35	0.47	0.24, 0.92	0.028*
Bilobar		10	1.63	0.80, 3.34	0.179			
Blood loss	59	41	1	1.00, 1.01	0.009*			
TBS	55	39	1.17	1.03, 1.32	0.014*			
HCC		8	0.62	0.28, 1.36	0.233	0.37	0.16, 0.89	0.026*
Others tumors		6	0.44	0.18, 1.08	0.074	0.23	0.08, 0.68	0.007*
R1/R2		10	3.21	1.55, 6.62	0.002*	3.78	1.66, 8.59	0.002*

OS, overall survival; HR, hazard ratio; CI, confidence interval; DFS, disease-free survival; TBS, tumor burden score; BMI, body mass index; 3D, three-dimensional; HCC, hepatocellular carcinoma.
*Statistically significant difference ($p < 0.05$).

[10,11,26-30].

Our findings suggest that anatomical factors, such as bilobar tumor distribution, and functional parameters, such as the ALBI score, are the primary determinants of achieving R0 resection in this cohort. In contrast, technical or demographic variables, including the use of 3D modeling, were not independently predictive.

In our multivariable analysis, bilobar tumor distribution and impaired hepatic function (indicated by a higher ALBI score) were identified as the strongest predictors of positive margins. This finding supports existing evidence that links these factors to restricted parenchymal reserve and a limited ability to achieve wide margins [20,31-33].

The role of the TBS deserves specific attention. Although TBS could not be integrated into multivariable models due to missing data in cases of pCCA and gallbladder carcinoma, it showed a significant association with recurrence in univariate analyses. This finding aligns with its established prognostic utility as a comprehensive measure of tumor size and number across hepatobiliary malignancies [19]. Its exclusion from the multivariable model indicates a methodological limitation rather than a lack of biological relevance. In larger datasets, TBS would likely continue to be a strong predictor of recurrence. Another notable finding is the inverse association between BMI and recurrence risk, which reflects the so-called "obesity paradox." Previous studies in general and hepatobiliary surgery have demonstrated that overweight or obese patients may experience postoperative and oncological outcomes that are equal to or even better than those of their normal-weight counterparts, despite their theoretical burden of comorbidities [34-36]. Guo et al. (2015) [36] specifically analyzed patients undergoing curative hepatectomy for HCC and found no significant differences in DFS at 1, 3, or 5 years between obese and non-obese patients. However, this effect should be interpreted cautiously.

The principal contribution of this study is that 3D modeling is independently associated with improved two-year DFS. The lack of statistical significance in the univariate analysis does not rule out an independent association in multivariable models, as adjusting for relevant confounders–such as tumor type, resection margin status, BMI, and intraoperative blood loss–may uncover effects that are obscured in unadjusted analyses. While unmeasured confounding and temporal effects cannot be completely ruled out, existing literature, despite its heterogeneity, supports the idea that 3D planning facilitates more accurate resections and enhances parenchymal-sparing strate-

gies, particularly in complex anatomical situations [10,11,27,37-39].

Although unmeasured confounding and temporal effects cannot be entirely ruled out, our findings indicate that the advantages of 3D modeling are more evident in medium-term oncological control than in immediate operative metrics like R0 rates. These results advocate for the use of 3D liver modeling as a tool to enhance oncological planning, particularly in anatomically complex cases where adequate parenchymal preservation is crucial. The observed reduction in recurrence points to its potential role in improving long-term outcomes beyond just technical execution. Integrating 3D models into standard preoperative workflows may be particularly beneficial for patients with bilobar or multifocal disease.

Tumor type was a significant determinant of recurrence, with HCC and other tumors showing a lower recurrence risk than CRLM. This finding aligns with existing evidence; contemporary studies report two-year recurrence rates exceeding 75% after the resection of CRLM, reflecting the systemic nature of colorectal cancer. In contrast, two-year recurrence rates after curative resection for HCC range from approximately 47% to 60%, even in patients with early-stage disease [40,41]. These differences in cumulative recurrence rates underscore the importance of tumor type as a key factor influencing short-term DFS after liver resection.

This study has inherent limitations due to its retrospective design. Notably, the before–after study design carries a significant risk of temporal bias, particularly following the mid-study introduction of 3D modeling. Factors such as improvements in surgical expertise, perioperative management, patient selection, and the increasing use of minimally invasive techniques may have independently influenced oncologic outcomes, separate from the effects of 3D planning. While baseline demographic and clinical characteristics were similar between groups for the measured variables, unmeasured changes in clinical practice and learning-curve effects cannot be ruled out. Additionally, although the use of 3D models was linked to improved two-year DFS, there was no corresponding increase in R0 resection rates, which limits causal interpretation. This suggests that the observed association may be due to indirect effects or residual confounding rather than a direct oncologic benefit of 3D planning. The inclusion of biologically diverse primary and metastatic liver tumors, which have distinct recurrence patterns, also poses a significant limitation that may impact the interpretation of survival analyses. Furthermore, the inability to include TBS–a well-established prognostic factor–in multivariable models due to missing data may have led to residual confounding, particularly in analyses of DFS. Finally, the relatively small sample size and the limited number of survival events, especially regarding OS, may have diminished statistical power and model stability. Therefore, the findings should be interpreted with caution and viewed as hypothesis-generating, necessitating validation in prospective, ideally randomized, studies.

FUNDING

None.

CONFLICT OF INTEREST

No potential conflict of interest relevant to this article was reported.

ORCID

María Victoria Vieiro Medina,
https://orcid.org/0000-0002-4421-1825
Laura Alonso Murillo,
https://orcid.org/0000-0002-8832-2404
Carlos Ernesto García Vasquez,
https://orcid.org/0000-0003-4177-7919
Victor Nieto Barros, https://orcid.org/0000-0002-3592-9288
Marta de la Fuente Bartolomé,
https://orcid.org/0000-0002-2932-1663
Fernando Neria, https://orcid.org/0000-0002-4417-2248
Santos Francisco Jiménez de los Galanes Marchán,
https://orcid.org/0000-0002-7087-9837

AUTHOR CONTRIBUTIONS

Conceptualization: MVVM. Data curation: MVVM. Methodology: FN. Visualization: MVVM. Writing – original draft: MVVM. Writing – review & editing: LAM, CEGV, VNB, MFB, SFJGM.

REFERENCES

1. Witowski JS, Pędziwiatr M, Major P, Budzyński A. Cost-effective, personalized, 3D-printed liver model for preoperative planning before laparoscopic liver hemihepatectomy for colorectal cancer metastases. Int J Comput Assist Radiol Surg 2017;12:2047-2054.
2. Igami T, Maehigashi A, Nakamura Y, Hayashi Y, Oda M, Yokoyama Y, et al. A clinical assessment of three-dimensional-printed liver model navigation for thrice or more repeated hepatectomy based on a conversation analysis. Surg Today 2024;54:1238-1247.
3. Liu JP, Lerut J, Yang Z, Li ZK, Zheng SS. Three-dimensional modeling in complex liver surgery and liver transplantation. Hepatobiliary Pancreat Dis Int 2022;21:318-324.
4. Rossi T, Williams A, Sun Z. Three-dimensional printed liver models for surgical planning and intraoperative guidance of liver cancer resection: a systematic review. Appl Sci 2023;13:10757.
5. Souzaki R, Kinoshita Y, Ieiri S, Hayashida M, Koga Y, Shirabe K, et al. Three-dimensional liver model based on preoperative CT images as a tool to assist in surgical planning for hepatoblastoma in a child. Pediatr Surg Int 2015;31:593-596.

6. Lopez-Lopez V, Robles-Campos R, García-Calderon D, Lang H, Cugat E, Jiménez-Galanes S, et al. Applicability of 3D-printed models in hepatobiliary surgey: results from "LIV3DPRINT" multicenter study. HPB (Oxford) 2021;23:675-684.
7. Bangeas P, Tsioukas V, Papadopoulos VN, Tsoulfas G. Role of innovative 3D printing models in the management of hepatobiliary malignancies. World J Hepatol 2019;11:574-585.
8. Perica ER, Sun Z. A systematic review of three-dimensional printing in liver disease. J Digit Imaging 2018;31:692-701.
9. Witowski JS, Coles-Black J, Zuzak TZ, Pędziwiatr M, Chuen J, Major P, et al. 3D printing in liver surgery: a systematic review. Telemed J E Health 2017;23:943-947.
10. Banchini F, Capelli P, Hasnaoui A, Palmieri G, Romboli A, Giuffrida M. 3-D reconstruction in liver surgery: a systematic review. HPB (Oxford) 2024;26:1205-1215.
11. Zeng L, Zhu Y, Guo P. Meta-analysis of the effects of three-dimensional visualized medical techniques hepatectomy for liver cancer with and without the treatment of sorafenib. Evid Based Complement Altern Med 2022;2022:4507673.
12. Lu Y, Chen X, Han F, Zhao Q, Xie T, Wu J, et al. 3D printing of self-healing personalized liver models for surgical training and preoperative planning. Nat Commun 2023;14:8447.
13. Fukumitsu K, Ishii T, Ogiso S, Yoh T, Uchida Y, Ito T, et al. Impact of patient-specific three-dimensional printed liver models on hepatic surgery safety: a pilot study. HPB (Oxford) 2023;25:1083-1092.
14. Vieiro Medina MV, Alonso Murillo L, García Vasquez CE, de la Fuente Bartolomé M, Nieto Barros V, Neria F, et al. Three-dimensional models in hepatic surgery: clinical outcomes a single-center experience. J Clin Med 2025;14:8659.
15. Neeman E, Gresham G, Ovasapians N, Hendifar A, Tuli R, Figlin R, et al. Comparing physician and nurse eastern cooperative oncology group performance status (ECOG-PS) ratings as predictors of clinical outcomes in patients with cancer. Oncologist 2019;24:e1460-e1466.
16. Sharara AI, Rockey DC. Gastroesophageal variceal hemorrhage. N Engl J Med 2001;345:669-681.
17. Daabiss M. American Society of Anaesthesiologists physical status classification. Indian J Anaesth 2011;55:111-115.
18. Wang YY, Zhong JH, Su ZY, Huang JF, Lu SD, Xiang BD, et al. Albumin-bilirubin versus Child-Pugh score as a predictor of outcome after liver resection for hepatocellular carcinoma. Br J Surg 2016;103:725-734.
19. Sasaki K, Morioka D, Conci S, Margonis GA, Sawada Y, Ruzzenente A, et al. The tumor burden score: a new "metro-ticket" prognostic tool for colorectal liver metastases based on tumor size and number of tumors. Ann Surg 2018;267:132-141.
20. Memeo R, de Blasi V, Adam R, Goéré D, Piardi T, Lermite E, et al.; French Colorectal Liver Metastases Working Group, Association Française de Chirurgie (AFC). Margin status is still an important prognostic factor in hepatectomies for colorectal liver metastases: a propensity score matching analysis. World J Surg 2018;42:892-901.
21. Zanon M, Altmayer S, Watte G, Pacini GS, Mohammed TL, Marchiori E, et al. Three-dimensional virtual planning for nodule resection in solid organs: a systematic review and meta-analysis. Surg Oncol 2021;38:101598.
22. Li L, Cheng S, Li J, Yang J, Wang H, Dong B, et al. Randomized comparison of AI enhanced 3D printing and traditional simulations in hepatobiliary surgery. NPJ Digit Med 2025;8:293.
23. Jiang J, Pei L, Jiang R. Clinical efficacy and safety of 3D vascular reconstruction combined with 3D navigation in laparoscopic hepatectomy: systematic review and meta-analysis. J Gastrointest Oncol 2022;13:1215-1223.
24. Kingham TP, Correa-Gallego C, D'Angelica MI, Gönen M, DeMatteo RP, Fong Y, et al. Hepatic parenchymal preservation surgery: decreasing morbidity and mortality rates in 4,152 resections for malignancy. J Am Coll Surg 2015;220:471-479.
25. Fonseca GM, Herman P, Faraj SF, Kruger JAP, Coelho FF, Jeismann VB, et al. Pathological factors and prognosis of resected liver metastases of colorectal carcinoma: implications and proposal for a pathological reporting protocol. Histopathology 2018;72:377-390.
26. Huber T, Huettl F, Tripke V, Baumgart J, Lang H. Experiences with three-dimensional printing in complex liver surgery. Ann Surg 2021;273:e26-e27.
27. Bonomi AM, Kersik A, Bracchetti G, Cotsoglou C. 3D reconstruction in complex parenchymal sparing liver surgery. Heliyon 2023;9:e13857.
28. Yang T, Lin S, Xie Q, Ouyang W, Tan T, Li J, et al. Impact of 3D printing technology on the comprehension of surgical liver anatomy. Surg Endosc 2019;33:411-417.
29. Cheng J, Wang Z, Liu J, Dou C, Yao W, Zhang C. Value of 3D printing technology combined with indocyanine green fluorescent navigation in complex laparoscopic hepatectomy. PLoS One 2022;17:e0272815.
30. Witowski J, Budzyński A, Grochowska A, Ballard DH, Major P, Rubinkiewicz M, et al. Decision-making based on 3D printed models in laparoscopic liver resections with intraoperative ultrasound: a prospective observational study. Eur Radiol 2020;30:1306-1312.
31. Tsim N, Healey AJ, Frampton AE, Habib NA, Bansi DS, Wasan H, et al. Two-stage resection for bilobar colorectal liver metastases: R0 resection is the key. Ann Surg Oncol 2011;18:1939-1946.
32. Wu CC, Ho WL, Lin MC, Yeh DC, Wu HS, Hwang CJ, et al. Hepatic resection for bilobar multicentric hepatocellular carcinoma: is it justified? Surgery 1998;123:270-277.
33. Xu FQ, Ye TW, Wang DD, Xie YM, Zhang KJ, Cheng J, et al. Association of preoperative albumin-bilirubin with surgical textbook outcomes following laparoscopic hepatectomy for hepatocellular carcinoma. Front Oncol 2022;12:964614.
34. Mullen JT, Moorman DW, Davenport DL. The obesity paradox: body mass index and outcomes in patients undergoing nonbariatric general surgery. Ann Surg 2009;250:166-172.
35. Akabane M, Kawashima J, Altaf A, Woldesenbet S, Cauchy F, Aucejo F, et al. Unraveling the obesity paradox in hepatocellular carcinoma: relative role of elevated body mass index on detrimental effects of postoperative complications. HPB (Oxford) 2025;27:1103-1112.
36. Guo Z, Zhang J, Jiang JH, Li LQ, Xiang BD. Obesity does not influence outcomes in hepatocellular carcinoma patients following curative hepatectomy. PLoS One 2015;10:e0125649.
37. Felli E, Boleslawski E, Sommacale D, Scatton O, Brustia R, Schwarz L, et al. Paradigm shift: should preoperative 3D reconstruction models

become mandatory before hepatectomy for hepatocellular carcinoma (HCC)? Results of a multicenter prospective trial. HPB (Oxford) 2023;25:293-300.
38. Nakayama K, Oshiro Y, Miyamoto R, Kohno K, Fukunaga K, Ohkohchi N. The effect of three-dimensional preoperative simulation on liver surgery. World J Surg 2017;41:1840-1847.
39. Panettieri E, Vega EA, Salirrosas O, Ogiso S, Geller D, Conrad C. Global practice patterns of preoperative image reconstruction for liver surgery. J Gastrointest Surg 2024;28:26-32.
40. Yao LQ, Chen ZL, Feng ZH, Diao YK, Li C, Sun HY, et al. Clinical features of recurrence after hepatic resection for early-stage hepatocellular carcinoma and long-term survival outcomes of patients with recurrence: a multi-institutional analysis. Ann Surg Oncol 2022;29:4291-4303.
41. de Jong MC, Pulitano C, Ribero D, Strub J, Mentha G, Schulick RD, et al. Rates and patterns of recurrence following curative intent surgery for colorectal liver metastasis: an international multi-institutional analysis of 1669 patients. Ann Surg 2009;250:440-448.